Title

On the force exerted on a non-spherical asymmetric dust grain from homogeneous, stationary, isotropic, non-magnetized plasma

Journal

Physics of Plasmas, 31(2)

ISSN

1070-664X

Authors

Krasheninnikov, SI

Smirnov, RD

Publication Date

2024-02-01

DOI

10.1063/5.0183855

On the force exerted on a non-spherical asymmetric dust grain from homogeneous, stationary, isotropic, non-magnetized plasma

S. I. Krasheninnikov and R. D. Smirnov*
University of California San Diego, Department of Mechanical and Aerospace Engineering
9500 Gilman Dr., La Jolla, CA 92093-0411, USA

*Corresponding author e-mail: rsmirnov@ucsd.edu

Abstract
Whereas the conventional wisdom suggests that the force between non-magnetized homogeneous, stationary, isotropic plasma and the dust grain is only possible for the case of relative plasma-grain velocity it is shown that stationary non-spherical asymmetric dust grain immersed into stationary, non-magnetized, isotropic plasma can experience a force caused by the grain-plasma interactions. The component of the force due to scattering of plasma particles in the limit of infinite Debye length is considered analytically. Both the particle scattering and absorption force components are modelled numerically in the limits of infinite and finite Debye length using newly developed 2D3V Aspherical Particle-in-Cell (APIC) code. The code simulates interactions of dust grain of selected non-spherical asymmetric shape with plasmas using dust shape conforming coordinates. The simulations confirm the existence of the force on non-spherical asymmetric grain in stationary non-magnetized plasma and show that the plasma screening effects can lead to reversal of the force direction.

1. Introduction

The dynamics of dust (micro-particles of an effective radius from nanometers to tens of microns) often is an important ingredient in different plasma-related phenomena in fusion devices, astrophysics, physics of the solar system, and laboratory experiments [1-6]. Therefore, there are many theoretical papers devoted to the studies of the forces and torques exerted on dust grains in the course of grain-plasma interactions (e.g. see [5-10] and the references therein). In most cases, these studies assumed spherical grain shapes, and such forces and torques were associated with an electric field, relative grain and plasma velocities, plasma temperature gradients, shear of plasma flow, gyro-motion of plasma electrons and ions, etc.

However, in practice, the shapes of natural dust grains are far from being spherical, e.g. see Refs. [1,4,5,7]. In this case, finding the forces and torques exerted on the grain from surrounding plasma becomes a challenge. In most of the available theoretical and computational studies, only charging processes were considered, see for example Refs. [11,12]. Very few publications exist analyzing forces on non-spherical grains in plasma that are largely concerned with relatively simple shapes of the grains in the forms of cylinder and prolate/oblate spheroids [13,14]. Although, angle dependencies of the ion absorption cross-section by some particle

agglomerates were simulated in [15] and dynamics of elongated fractal-like water-ice particles were experimentally studied in work [16].

Yet, an approach based on the consideration of some particular shapes of the grains lacks generality and for this reason has rather limited application range. Therefore, it makes sense to use more general properties of the dust shape and build up a theory of grain dynamics based on these properties. In this case one could only account for the features of the shape essential for the description of the grain dynamics. Such a theory was developed in Refs. [17,18], where an approach utilizing the moments attributed to the shape of the grain combined with different coordinate transformation properties of polar- and pseudo-vectors was used. We notice that a similar approach was used in the studies of the dynamics of small particles embedded into fluids [19,20]. However, in Ref. [17] it was *a priory* assumed that there are no forces and torques on non-spherical grains in stationary plasma and the corresponding zero-order terms in relation to relative grain-plasma translational and rotational velocities were missing in the proposed model.

In this paper we extend the general theoretical consideration of forces acting on non-spherical dust in plasma to the case of homogeneous, stationary, non-magnetized plasma. We demonstrate both theoretically and computationally that forces exerted on the non-spherical asymmetric grain from plasma appear to exist even at zero relative dust-plasma velocity due to interactions of plasma particles with asymmetric electric field associated with the grain shape non-sphericity.

2. Theoretical consideration of scattering force on non-spherical asymmetric dust

We consider a grain having rotational symmetry around the z-axis, but asymmetric in the z-direction (see Fig. 1). The spatial orientation of such asymmetric grain can be characterized by the unit vector $\vec{D}$. Assume now that this grain is embedded into non-magnetized plasma and the relative plasma-grain velocity is $\vec{U}_d$. In case the grain is not spinning, the force, $\vec{F}_d$, acting on the grain should be expressed with the vectors $\vec{D}$ and $\vec{U}_d$ and some scalar quantities characterizing both plasma (e.g. density, n, and temperature, T) and the dust grain (e.g. grain effective size R_d). Keeping in mind that $\vec{F}_d$ is a polar vector in the lowest order over velocity U_d ($U_d \ll C_s \equiv \sqrt{T_e/M_i}$, where M_i is the ion mass and T_e is the electron temperature, which as assume is larger than the ion one, T_i) we find

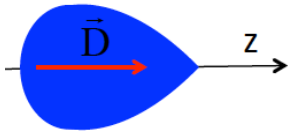

Fig. 1. *Schematic view of non-spherical dust grain having rotational symmetry around z-axis but asymmetric in z-direction.*

$$\vec{F}_d = \Phi_D \vec{D} + \Phi_U \vec{U}_d + \Phi_{UD} \vec{D}\left(\vec{U}_d \cdot \vec{D}\right), \qquad (1)$$

where Φ_D, Φ_U, and Φ_{UD} are the constant scalars depending on both plasma and dust grain parameters. Even though an exact calculation of these scalars is a difficult problem, some rather

simple estimates of $_U$ and $_{UD}$, allowing shed light on the dynamics of non-spherical asymmetric dust grains, can be made [5,17,18]. For grain shapes not very different from spherical, the simple dimensional considerations give the magnitude of the force acting on the non-spinning grain due to plasma flow with the relative velocity $U_d \ll C_s$ as $F_{est} \sim \xi_F \pi R_d^2 n T U_d / C_s$, where $\xi_F \sim 10$ is the form factor depending on the ratio of the Debye length to the grain size. Then, assuming that the center of force and the grain's center of mass are displaced by a distance $\sim R_d$, the scalar coefficients can be approximated as $\Phi_U \sim \Phi_{UD} \sim F_{est}/U_d \sim \xi_F \pi R_d^2 n T / C_s$ [17].

As we see from Eq. (1) the formal expression for the force implies that the force, caused by grain-plasma interactions, could be exerted on the grain even by stationary plasma, notice the first term on the right-hand side of Eq. (1). For the case of fluid described by Navier-Stokes equations, it is easy to show that $_D = 0$ and such force does not exist. Indeed, taking into account that both the fluid and the grain are stationary, we have $\Phi_D \vec{D} = -\oint_{S_d} p \, d\vec{S} = 0$, where p is the pressure and the integration goes over the entire grain surface, S_d (e.g. see Ref. 19, 20). However, in what follows we will consider the collisionless plasma, the interaction of which with the grain cannot be described with the Navier-Stokes equations and, therefore, $_D$ could be finite.

Indeed, recently, it was found that in the case of non-spherical asymmetric stationary grain situated in stationary plasma embedded into a magnetic field $\vec{B}$, the $\vec{j} \times \vec{B}$ force (where $\vec{j}$ is the electric current flowing through the grain) could exist [21].

We notice that in the case of inhomogeneity of the surface material properties, the forces due to asymmetry of material ablation or the accommodation of the momenta of electrons and ions impinging to the surface exist even for a spherical grain immersed into non-magnetized plasma. But, in what follows we will not consider such effects. Instead, we will present the arguments, supported by numerical simulations, that for the case of interaction of non-spherical asymmetric conducting grain with collisionless plasma $_D$ can be finite even for no grain ablation and homogeneous surface material.

For the illustration we take the grain shape corresponding to the "equipotential" equation for the combination of the charge and a dipole, written in spherical coordinates (described by the radius vector $\vec{r}$ and the angle between $\vec{r}$ and the dipole axis)

$$1 = \frac{R_d}{r} + \cos( ) \left(\frac{R_d}{r} \right)^2, \qquad (2)$$

where is the dimensionless strength of a dipole and R_d is the characteristic size of the grain. Solving Eq. (2) for the radius r as the function of the angle we find the following expression

$$r = \frac{R_d}{2} \left(1 + \sqrt{1 + 4 \cos( )} \right), \qquad (3)$$

which shows that the surface of the grain determined by Eq. (2) has the "closed shell" form for $|\ |<1/4$.

Since the grain material is a conductor the grain surface is equipotential. Then, assuming that the Debye length, $_D$, is significantly larger than the characteristic size of the dust grain R_d, the distribution of the electrostatic potential, $\varphi(\vec{r})$, in the vicinity of the grain, $R_d \lesssim r < \lambda_D$, can be approximated as

$$\varphi(\vec{r}) = \varphi_d\left[\frac{R_d}{r} + \delta\cos(\vartheta)\left(\frac{R_d}{r}\right)^2\right], \tag{4}$$

where φ_d is the grain surface potential.

To illustrate that the net z-component of momentum transfer to the dust grain from the stationary plasma can be finite, we consider the dynamics of two trace particles moving in the electrostatic potential (4) and having charge q and mass M. As a result, the interaction of these particles with the grain is described by the potential energy

$$U(\vec{r}) = U_0\left(\frac{R_d}{r} + \delta\cos(\vartheta)\left(\frac{R_d}{r}\right)^2\right), \tag{5}$$

where the constant $U_0 = q\varphi_d$, depending on sign of q and φ_d, can be both positive and negative. We assume that these particles are approaching the grain parallel to the z-direction from $z = \pm\infty$ (e.g. see Fig. 2) and have the same target parameter, , and speed, $|\vec{V}_\infty|$.

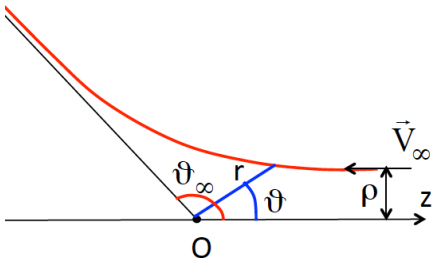

Fig. 2. *Scattering of a trace particle.*

Using the expression (5) we find the force exerted on the trace particle, $\vec{F} = -\nabla U(\vec{r})$, and obtain the following equation for the particle axial component of angular momentum, L_z:

$$\frac{dL_z}{dt} \equiv \frac{d}{dt}\left(Mr^2\frac{d}{dt}\right) = U_0\left(\frac{R_d}{r}\right)^2 \sin \quad . \tag{6}$$

Multiplying Eq. (6) by L_z and integrating over time we find

$$L_z^2 \equiv \left(Mr^2\frac{d}{dt}\right)^2 = \left(M\ V_\infty\right)^2 \quad 2MU_0\ R_d^2\left(\cos \quad 1\right), \tag{7}$$

which gives

$$\frac{d}{dt} = \pm\frac{V_\infty}{r^2}\left\{1 + 2\ \frac{U_0}{MV_\infty^2}\left(\frac{R_d}{r}\right)^2\left(1\ \cos\ \right)\right\}^{1/2}, \tag{8}$$

Substituting Eq. (8) into the energy conservation equation, $M\left(\dot{r}^2 + r^2\dot{\vartheta}^2\right)/2 + U(\vec{r}) = MV_\infty^2/2$, we find

$$\frac{dr}{dt} = \pm V_\infty \left\{1 - 2\frac{U_0}{MV_\infty^2}\frac{R_d}{\rho}\frac{\rho}{r} - \left(\frac{\rho}{r}\right)^2\left[1 + 2\delta\frac{U_0}{MV_\infty^2}\left(\frac{R_d}{\rho}\right)^2\right]\right\}^{1/2}. \quad (9)$$

We notice that the difference in the scattering angles of the particles approaching the "scattering center" from $z = -\infty$ and $z = +\infty$, can be found by changing the sign of .

Then, by dividing Eq. (8) by Eq. (9) we find

$$\left\{1+2\frac{U_0}{MV_\infty^2}\left(\frac{R_d}{}\right)^2\left(1\ \cos\ \right)\right\}^{1/2} d\ = \frac{}{r^2}\left\{1\ \ 2\frac{U_0}{MV_\infty^2}\frac{R_d}{}\frac{}{r}\ \left(\frac{}{r}\right)^2\left[1+2\ \frac{U_0}{MV_\infty^2}\left(\frac{R_d}{}\right)^2\right]\right\}^{1/2} dr \Rightarrow, \quad (10)$$

$$\int_0^\infty \frac{d}{\sqrt{1+[b/(1+b)]\cos(\ )}} = 2\arccos\left\{\frac{a}{\sqrt{1+b+a^2}}\right\}$$

where $_\infty$ is the scattering angle, $_\infty =$ $(t \to \infty)$. In Eq. (10) we use the results of the derivation of the Rutherford's formula from [22]. The constants a and b are defined as follows

$$a = \frac{2U_0}{MV_\infty^2}\frac{R_d}{\rho}, \qquad b = \frac{R_d}{}a. \quad (11)$$

It is well known that the main Coulomb drag force comes from the scattering on small angles, which implies $\to\infty$ and $_\infty \approx$. However, we are interested in plasma-grain momentum transfer for the case of no grain-plasma relative velocities. In this case the only reason for net momentum transfer can be asymmetry in scattering of plasma particles coming from $z = -\infty$ and $z = +\infty$ caused by the dipolar contribution into potential (5) and related to the parameter b in Eq. (10).

Since the goal of this analytic consideration is just the illustration of the momentum transfer due to asymmetry of the grain, we consider an impact of asymmetric scattering for $>>R_d$, which implies that $a << 1$, and assume that $b \propto \ \to 0$. For this case from Eq. (10), we find the following expansion of the scattering angle in the Taylor series over parameter $b \propto \ \to 0$

$$_\infty(\ ) \approx \quad 2a\ \ \frac{15}{64}\ b^2 + \frac{35}{(16)^2}\ b^3. \quad (12)$$

Notably, the term proportional to $b\mu$ does not exist in this expansion. The first two terms on the right-hand side of Eq. (12) describe a "standard" Coulomb small angle scattering (see the derivation of the Rutherford's formula in [22]). The third and fourth terms on the right-hand side of Eq. (12) describe the contribution of the dipolar part, μ, of the electrostatic potential (4). However, the third term is proportional to ^{2} and, therefore, does not depend on the sign of . As a result, its contribution to the momentum transfer of the particles approaching the "scattering center" from $z = -\infty$ and $z = +\infty$ cancels. Thus, only fourth term on the right-hand side of Eq. (12) proportional to ^{3} describes an impact of asymmetry on the scattering of the particles approaching the "scattering center" from $z = -\infty$ and $z = +\infty$, and contributes to the plasma-grain momentum transfer.

As a result, the net z-components of the momentum transfer, P_z, from two particles, having the same initial energy $MV_\infty^2/2$ and the target parameter , but approaching the "scattering center" from different directions, $z = -\infty$ and $z = +\infty$ is:

$$P_z \propto MV_\infty \left\{ \cos\left(\quad (\quad) \right) \quad \cos\left(\quad (\quad) \right) \right\} \approx \frac{35}{32} \; MV_\infty \left(\frac{R_d}{} \right)^3 \left(\frac{2U_0}{MV_\infty^2} \frac{R_d}{} \right)^4 . \qquad (13)$$

However, the expression (13) can only serve as an illustration of an impact of asymmetric (dipolar) term in the shape of the grain on the net plasma-grain momentum exchange. Indeed, by examining the expression (13) we find that such momentum exchange is dominated by "small" target parameter and, therefore, large angle scattering (this contrary to a "standard" drag force determined by large and small angle scattering [22]). As a result, total force exerted on the grain also should account for the collisions of plasma particles with the grain, which goes beyond what can be done analytically. In addition, one also should take into account the Debye screening effects. All of these can only be done numerically.

3. Modeling of forces acting on unscreened grain

First, to verify the results of the theoretical considerations above and evaluate the forces due plasma particles scattering and collection by dust, we simulate trajectories of electrons and ions in a fixed field of charged non-spherical asymmetric grain neglecting the interactions between the plasma particles themselves. This approximation corresponds to the limit of $\lambda_D \gg R_d$ considered in the Section 2.

Here we consider negatively charged conducting dust grain with shape corresponding to the equipotential surface $\varphi_d \cong -2.16\, T_e/e$ described by Eq. (2) with $R_d = 10\mu m$ and $\delta = -0.24$. The simulated trajectories start at an equipotential outer boundary surface corresponding to unscreened potential $\varphi_b = \varphi_d/10$. The injected electrons and ions have Maxwellian velocity distributions with particle density $n = 5.5 \cdot 10^{17}\ m^{-3}$, electron and ion temperatures equal $T_e = 1.0$ eV and $T_i = 0.3$ eV, respectively. Here, we assumed ions to be deuterium and electron to ion mass ratio $M_e/M_i = 0.01$. The electron and ion trajectories are tracked in the analytically

calculated field of the grain with time step 10^{-11} s until they cross either the grain's surface or the outer boundary. Then, the momentum lost by the plasma particles either due to scattering or absorption by the grain is accumulated over time and used to calculate time-averaged electric and absorption forces acting on the grain, respectively.

	$F_E/(\pi R_d^2 n T_e)$	$F_{abs}/(\pi R_d^2 n T_e)$
electrons	$1.2 \cdot 10^{-4} \pm 6 \cdot 10^{-5}$	$1 \cdot 10^{-5} \pm 1 \cdot 10^{-5}$
ions	$-2.81 \cdot 10^{-3} \pm 2.4 \cdot 10^{-4}$	$1.2 \cdot 10^{-4} \pm 1.7 \cdot 10^{-4}$

Table 1. *Simulated normalized electric and absorption forces exerted on the non-spherical asymmetric grain by electrons and ions for the unscreened grain field case.*

For the simulated accumulation time equal $\sim 2.5 \cdot 10^{-4}$ s, we obtain the electric force F_E and the absorption force F_{abs} exerted on the grain by electrons and ions that are shown in Table 1. The negative value indicates that a force is directed from the "dull" to the "sharp" end of the grain, antiparallel to its dipole moment direction. The uncertainty intervals are calculated as standard deviation of the mean using values of the forces obtained at every timestep. We can see that the forces exerted by electrons are negligible even for the simulated relatively large M_e/M_i ratio. Also, the force due to absorption of ions by the grain is near zero within the simulation uncertainty. Notably, the ion scattering force has the sign and the magnitude roughly in accord with the theoretical evaluation, Eq. (13), where $F_E^i/(\pi R_d^2 n T_e) = -2.81 \cdot 10^{-3} \sim (T_i/T_e)\delta^3 = -4.15 \cdot 10^{-3}$.

Therefore, these simulations extend the above analytical considerations to the case of Maxwell distributed ensemble of plasma particles and support existence of the force exerted on the unscreened non-spherical asymmetric grain by ions with non-flowing unperturbed distribution function. They also indicate that the role of absorption is negligible in this case.

4. Modelling of forces acting on plasma screened grain

To simulate interactions of the non-spherical asymmetric grain with plasma including effects of plasma screening, we developed the 2D3V Aspherical Particle-in-Cell (PIC) code "APIC". The APIC code uses electrostatic PIC method [23,24] for modeling of plasma particles motion in a self-consistent electric field. The 2D3V APIC code can model rotationally symmetric systems that include a conductive non-spherical dust grain in the middle.

The simulated system setup is analogous to that of Section 3, where the boundaries of the modelled system are selected to correspond to the surface of the grain and the unscreened equipotential surface external to the grain. The grain surface has fixed potential, the same as in the unscreened case, and the system's outer boundary potential is now set to zero, while the system's radial size is equal $\sim 10\lambda_D$. Plasma particles are injected into the system through the outer boundary with non-shifted Maxwellian velocity distribution function.

To significantly reduce errors associated with the electric field calculations at the grain surface we introduce dimensionless, dust-shape-conforming curvilinear coordinates (x_1, x_2) in APIC code as follows:

$$x_1 = -\frac{R_d}{r}\left(1 + \frac{\delta R_d \cos\theta}{r}\right),\ x_2 = \cos\theta. \tag{14}$$

Inverse transformation of the coordinates can also be expressed analytically:

$$r = -\frac{1+\sqrt{1-4\delta x_1 x_2}}{2x_1} R_d,\ \theta = \arccos x_2. \tag{15}$$

We note that the conforming coordinates (x_1, x_2) are non-orthogonal. The surface of the dust grain corresponds to constant $x_1 = -1$ and the simulated system's outer boundary to some arbitrarily selected constant value $-1 < x_1 < 0$. Then, the differential element of surface area corresponding to a constant x_1 can be expressed as

$$dA = 2\pi r^2 \sqrt{1 + (1 - x_2^2)\left(\frac{\delta R_d}{r + 2\delta R_d x_2}\right)^2}\, dx_2, \tag{16}$$

and the differential volume element as

$$d\Omega = \frac{2\pi r^5}{R_d(r + 2\delta R_d x_2)} dx_1 dx_2, \tag{17}$$

which are used in APIC code for the charge distribution on the grid and the plasma particle injection purposes. The Poisson's equation for potential φ in the domain with plasma charge density ρ_{pl} is

$$\triangle_{x_1,x_2}\, \varphi(x_1, x_2) = -4\pi\rho_{pl}(x_1, x_2), \tag{18}$$

where Laplace operator in the curvilinear coordinates has form

$$\triangle_{x_1,x_2} = \frac{(r/R_d + 2\delta x_2)^2 + \delta^2(1-x_2^2)}{(r/R_d)^6}\frac{\partial^2}{\partial x_1^2} + \frac{1-x_2^2}{(r/R_d)^2}\frac{\partial^2}{\partial x_2^2} - \frac{2\delta(1-x_2^2)}{(r/R_d)^4}\frac{\partial^2}{\partial x_1 \partial x_2} - \frac{2x_2}{(r/R_d)^2}\frac{\partial}{\partial x_2}. \tag{19}$$

For simplicity of interpretation and possibility to generalize simulations to other curvilinear coordinates, we describe dynamics of plasma particles using dimensional cylindrical coordinates (R, Z), where

$$R = r\sqrt{1 - x_2^2},\ Z = r x_2. \tag{20}$$

A constant magnetic field B parallel to the rotational symmetry axis in general can be present in the modelled system. In this case, Lorentz force acting on plasma particles is also calculated in APIC code. In this work, however, we consider only the case of $B = 0$. Corresponding equations of motion solved in the code for a plasma particle are

$$\begin{cases} \frac{dR}{dt} = V_R, \ \frac{dZ}{dt} = V_Z, \\ \frac{dV_R}{dt} = \frac{q}{M}(E_R - V_\Theta B) + \frac{V_\Theta^2}{R}, \ \frac{dV_Z}{dt} = \frac{q}{M}E_Z, \ \frac{dV_\Theta}{dt} = \frac{q}{M}V_R B - \frac{V_R V_\Theta}{R}. \end{cases} \tag{21}$$

In addition, to avoid numerical issues related to the singularity in the equations of motion when $R \to 0$, we solve the equations for V_R and V_Θ for each plasma particle in local cartesian coordinates that are coincident with R and Θ directions at position of a particle at previous time step. The electric field components in the cylindrical coordinates can be found from a solution of Eq. (18) for potential $\varphi(x_1, x_2)$, as follows

$$E_R = -\frac{\partial x_1}{\partial R}\frac{\partial \varphi}{\partial x_1} - \frac{\partial x_2}{\partial R}\frac{\partial \varphi}{\partial x_2},\ E_Z = -\frac{\partial x_1}{\partial Z}\frac{\partial \varphi}{\partial x_1} - \frac{\partial x_2}{\partial Z}\frac{\partial \varphi}{\partial x_2}. \tag{22}$$

We note that in Eq. (22) we find the derivatives of the potential numerically at the grid nodes with subsequent interpolation to a plasma particle position, while the coordinate derivatives are found analytically for arbitrary spatial coordinates. The electric field calculated on the boundary corresponding to the conducting grain surface is used to find the surface charge density from the normal field component and the electric force acting on the grain. The plasma currents, drag force due to plasma particles absorption, torques, and heat fluxes are computed, correspondingly, as plasma particles' charge, momentum, angular momentum, and energy transferred to the dust in unit time interval. The APIC code also has capability to model Boltzmann distributed electrons, in which case electron motion is not simulated and, instead, electron density is calculated as $n_e = n\exp(-e\varphi/T_e)$.

The equations of motion (21) are integrated in time using explicit leapfrog first order method. The simulation grid is selected to be uniform in curvilinear coordinates (x_1, x_2), on which finite difference derivatives are calculated to the second order precision. Then, a linear system of the finite difference equations corresponding to Poisson's equation (18) is solved using LU matrix decomposition routines from BLAS/LAPACK libraries. The code is written in Fortran and parallelized using OpenMP techniques.

APIC code has been validated in several ways, in particular, numerical solutions for unscreened dust field matched the analytical expressions and modeling of spherical dust grain showed no forces acting on it within statistical noise error, as expected (see more details on the code validation in the Appendix).

We performed simulations for the screened, non-spherical, asymmetric, negatively charged, conducting grain with $R_d = 10\ \mu m$, $\varphi_d \cong -2.16\,T_e/e$, and $\delta = -0.24$ in a plasma with unperturbed density $n = 5.5\cdot 10^{17}\ m^{-3}$, electron to ion mass ratio $M_e/M_i = 0.1$, and electron and ion temperatures equal $T_e = 1.0\ eV$ and $T_i = 0.1\ eV$, respectively. Due to the relatively small size of the simulated system, we were able to simulate plasma particle dynamics using the number of macro-particles representing the real number of electrons and ions in the system. That is initially equal $\sim 2.3\cdot 10^6$ particles of each sort in the uniformly filled simulation domain. The simulations used the uniform 500×1000 grid in (x_1, x_2) space and the integration time step $2.5\cdot 10^{-11}$ s.

$F_E/(\pi R_d^2 n T_e)$	$F_{abs}/(\pi R_d^2 n T_e)$
$4.8\cdot 10^{-4} \pm 3.5\cdot 10^{-4}$	$1.24\cdot 10^{-3} \pm 2.0\cdot 10^{-4}$

Table 2. *Simulated normalized electric and absorption forces on the non-spherical asymmetric grain exerted by plasma for the screened grain field case.*

The obtained electric force and the drag force due to plasma particles scattering and absorption by the grain, averaged over the simulated time $\sim 1.7\cdot 10^{-4}$ s, are shown in table 2. One can see that in this case the absorption force dominates and has a positive sign (parallel to the grain's dipole moment) that is opposite to the dominant electric force produced by ions in the unscreened grain case. Such effects, thus, should be attributed to the plasma screening that alters

potential distribution and correspondingly the plasma particles' trajectories around the grain, especially near its surface.

The effect of plasma screening is illustrated in Fig. 3, where the distribution of the plasma charge density ρ is plotted. One can see that the positive plasma charge accumulated near both axial ends of the grain ($x_2 = \pm 1$). When integrated over the plasma volume the total plasma charge and the plasma dipole moment both are opposite in sign and approximately half of the corresponding values of the grain, producing substantial plasma screening effect on the electric potential profile. The difference between the screened non-spherical dust potential, φ, and potential, φ_{sp}, simulated for screened spherical grain ($\delta = 0$) under the same conditions is plotted in Fig. 4. It demonstrates residual asymmetry of the potential distribution resulting from asymmetric charge accumulation near the axis of the non-spherical asymmetric grain. The screening would significantly affect ion trajectories and further shrink the region of large angle plasma particle scattering to close proximity of the grain's surface. This can possibly lead to the observed reduction and reversal of the scattering force on the non-spherical asymmetric grain as compared to the unscreened case.

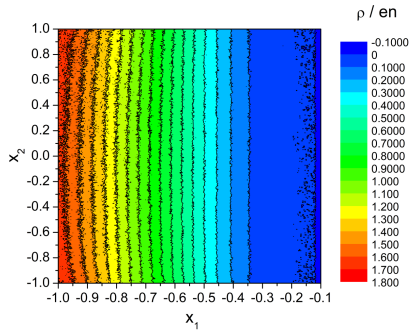

Fig. 3. *Simulated distribution of the plasma charge density for the screened non-spherical asymmetric grain case.*

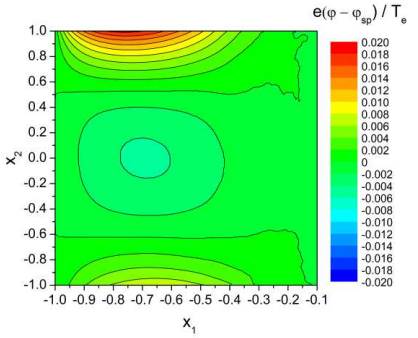

Fig. 4. *Simulated distribution of the difference between screened electric potentials for non-spherical and spherical grains.*

5. Conclusion

The developed general theoretical framework for description of dynamics of non-spherical asymmetric dust in plasmas suggests that there can exist forces on a non-spherical asymmetric grain in homogeneous, stationary, non-magnetized plasma arising due to scattering and collection of plasma particles moving in the asymmetric electric field of the grain. The presented analytical consideration for the specific case of probe particle scattering in the electric field of a charged grain having a dipolar component further strengthens the assertion of the scattering force existence and indicates that the force is proportional to the cube of the grain's dipole moment. The newly developed Aspherical Particle-in-Cell (APIC) code allows to evaluate the very small

plasma scattering and absorption forces acting on the non-spherical asymmetric grain. The numerical simulations confirm the ion scattering force existence in the case of unscreened grain having both unipolar and dipolar electric field components. The APIC modeling of the plasma screened grain indicates that the absorption force dominates the scattering one and has a reverse direction in comparison to the scattering force in the unscreened grain case. The force reversion due to the plasma screening underlines the complexity of the problem of plasma interactions with non-spherical asymmetric dust grains. Furthermore, a grain with shape having helical features may experience, besides the forces, also torques in the considered plasmas, which would require full three-dimensional treatment. The advocated in this work existence of the forces on non-spherical asymmetric grain in homogeneous, stationary, isotropic, non-magnetized plasma opens a new venue of the dust-plasma interaction research and may have far reaching implications when generalized to other interactions involving asymmetrically shaped objects.

Appendix

The APIC code's numerical solver of Poisson's equation (18) using Laplace operator (19) in the curvilinear transformed coordinates was verified for the case of non-spherical grain in vacuum $\rho_{pl} = 0$, for which the analytical solution of the potential around the non-spherical grain can be expressed as $\varphi(x_1, x_2) = -\varphi_d x_1$. For the non-spherical grain with the same parameters as modelled above the absolute difference between the numerical and analytical potential solutions, $\Delta\varphi_{err}$, is plotted in Fig. 5. One can see that the absolute numerical error of the potential does not exceed $\pm 5 \cdot 10^{-6}\, T_e/e$ that is several orders of magnitude smaller than the difference between potentials for the non-spherical and spherical grains plotted in Fig. 4. We also note that the numerical error of the potential solver, Fig. 5, does not depend on coordinate x_2 and its pattern is defined by the used linear algebra routines.

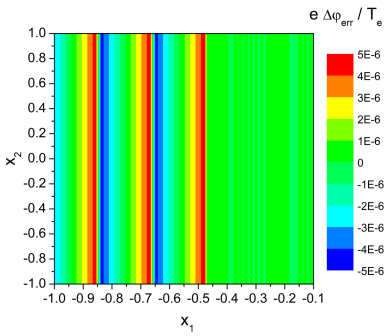

Fig. 5. *Simulated distribution of the difference between the numerical and analytical potential solutions for the non-spherical dust grain in vacuum.*

The APIC code was validated by modeling electric and particle absorption forces acting on spherical grain immersed in stationary plasma. The modeling parameters were the same as used above for the plasma screened grain but $\delta = 0$ was set corresponding to spherical grain shape. Table 3 shows the obtained electric and absorption forces on the grain, averaged over the simulated time $\sim 1.7 \cdot 10^{-4}$ s. As expected, the forces are near zero within the statistical error of the simulations. We note that the statistical error in this case is the same as for the screened non-spherical grain simulations due to the similar simulation parameters.

$F_E/(\pi R_d^2 n T_e)$	$F_{abs}/(\pi R_d^2 n T_e)$
$2.7 \cdot 10^{-4} \pm 3.5 \cdot 10^{-4}$	$1.1 \cdot 10^{-4} \pm 2.0 \cdot 10^{-4}$

Table 3. *Simulated normalized electric and absorption forces on the spherical grain exerted by plasma for the same plasma conditions as in the modelled screened non-spherical grain case.*

Acknowledgements

This material is based upon the work supported by the U.S. Department of Energy, Office of Science, Office of Fusion Energy Sciences under Award No. DE-FG02-06ER54852.

References

[1] L. Spitzer, "Physical Processes in the Interstellar Medium", Wiley, New York, 1978.
[2] C. K. Goertz, "Dusty plasma in the solar system", Rev. Geophys. **27** (1989) 271-292.
[3] D. A. Mendis and M. Rosenberg, "Cosmic dusty plasma", Ann. Rev. Astron. Astrophys. **32** (1994) 419-463.
[4] J. Winter, "Dust in fusion devices - experimental evidence, possible sources and consequences", Plasma Phys. Contr. Fusion **40** (1998) 1201-1210.
[5] S. I. Krasheninnikov, R. D. Smirnov, D. L. Rudakov, "Dust in magnetic fusion devices", Plasma Phys. Contr. Fusion **53** (2011) 083001.
[6] S. Ratynskaia, A. Bortolon, S. I. Krasheninnikov, "Dust and powder in fusion plasmas: Recent developments in theory, modeling, and experiments", Reviews Mod. Plasma Phys. **6** (2022) 20.
[7] P. K. Shukla, A. A. Mamun, "Introduction to Dusty plasma Physics", IoP, Bristol, 2002.
[8] I. H. Hutchinson, "Collisionless ion drag force on a spherical grain", Plasma Phys. Contr. Fusion **48** (2006) 185-202.
[9] P. K. Shukla, B. Eliasson, "Colloquium: Fundamentals of dust-plasma interactions", Rev. Mod. Phys. **81** (2009) 25-44.
[10] G. E. Morfill and A. V. Ivlev, "Complex plasmas: An interdisciplinary research field", Rev. Mod. Phys. **81** (2009) 1353-1404.
[11] J. T. Holgate and M. Coppins "Charging of nonspherical macroparticles in a plasma", Physical Review E **93** (2016) 033208.
[12] G. I. Sukhinin, A. V. Fedoseev, and M. V. Salnikov "The influence of dust particle geometry on its charge and plasma potential", Contributions to Plasma Physics **59** (2019) e201800153.
[13] A. V. Ivlev, A. G. Khrapak, S. A. Khrapak, B. M. Annaratone, G. Morfill, and K. Yoshino, "Rodlike particles in gas discharge plasmas: Theoretical model", Phys. Rev. E **68** (2003) 026403.
[14] S. I. Krasheninnikov and D. A. Mendis, "On the drag force on non-spherical dust grain", J. Plasma Phys. **77** (2011) 271-276.

[15] E. R. Keiter and M. J. Kushner, "Plasma transport around dust agglomerates having complex shapes", J. Appl. Phys. **83** (1998) 5670-5677.
[16] K-B Chai, "Dynamics of nonspherical, fractal-like water-ice particles in a plasma environment", Sci. Reports **8** (2018) 15405.
[17] S. I. Krasheninnikov, "On the dynamics of nonspherical dust grain in plasma", Phys. Plasmas **17** (2010) 033703.
[18] S. I. Krasheninnikov, "On the dynamics of propeller-like dust grain in plasma", Phys. Plasmas **20** (2013) 114502.
[19] H. Brenner, "The Stokes resistance of an arbitrary particle", Chem. Eng. Science **18** (1963) 1-25.
[20] H. Brenner, "The Stokes resistance of an arbitrary particle - II An extension", Chem. Eng. Science **19** (1964) 599-629.
[21] S. I. Krasheninnikov, "On the force exerted on a non-spherical dust grain from homogeneous magnetized plasma", Phys. Plasmas **30** (2023) 040701.
[22] L. D. Landau, and E. M. Lifshits, 2003 *Course of Theoretical Physics, Vol. 1 Mechanics*. Amsterdam, The Netherlands: Elsevier.
[23] C. K. Birdsall and A. B. Langdon, "Plasma Physics via Computer Simulation", (New York: McGraw-Hill, 1985).
[24] R. W. Hockney and J. W. Eastwood, "Computer Simulation using Particles", (New York: Taylor & Francis Group, 1988).

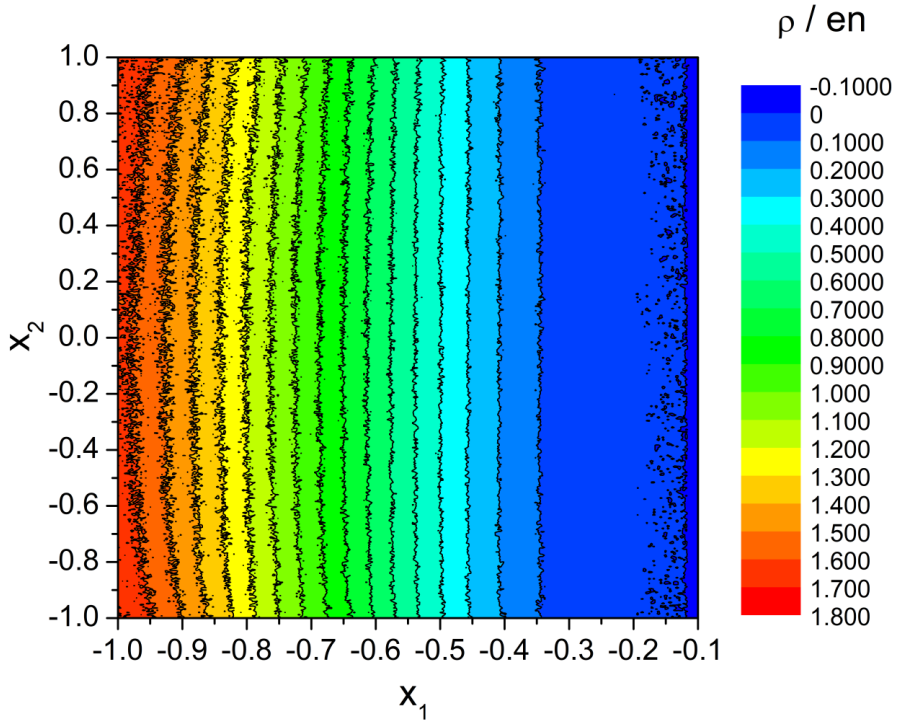

Fig. 3

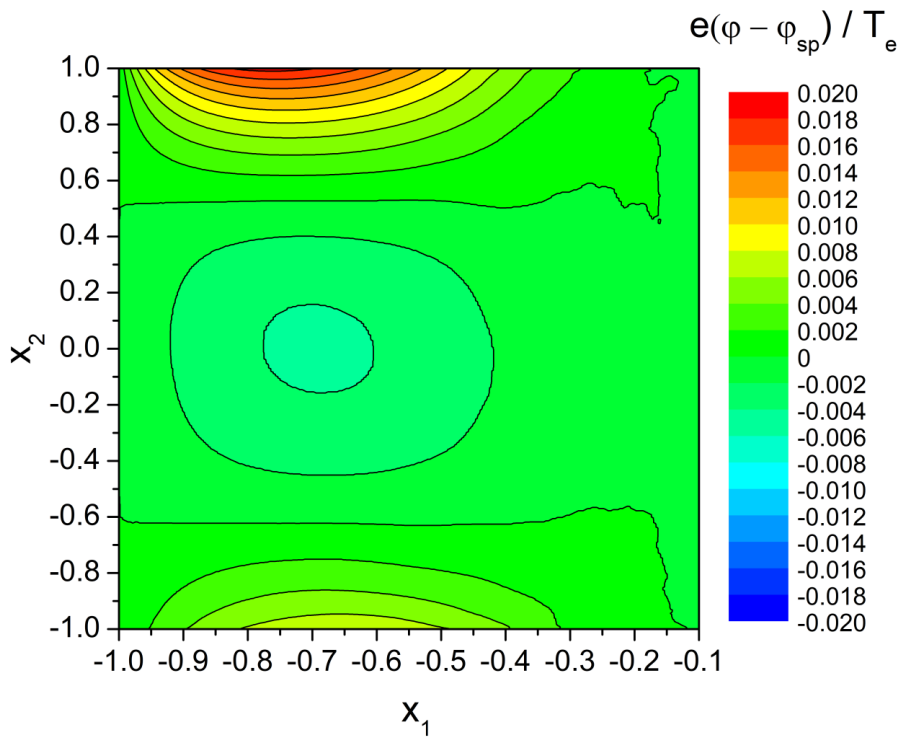

Fig. 4

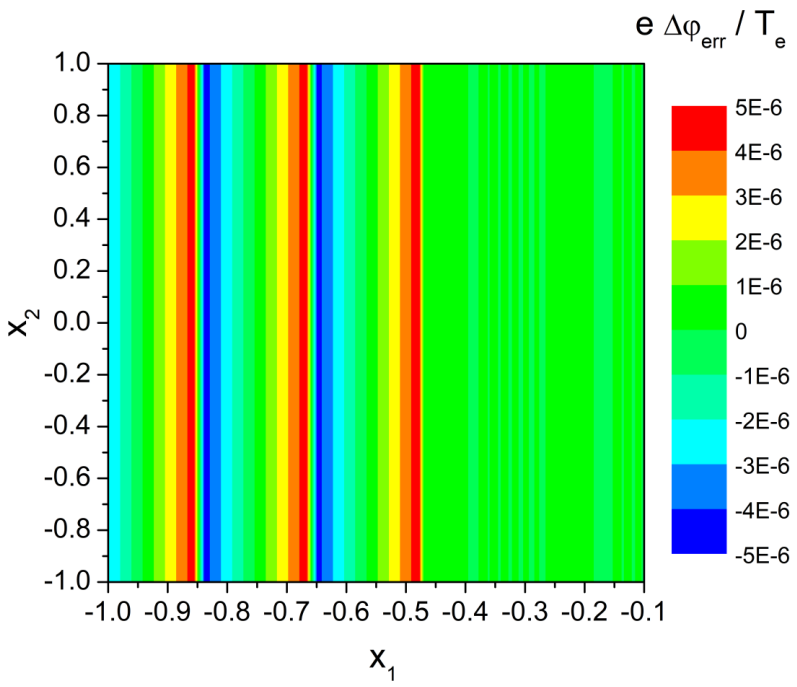

Fig. 5